ELSEVIER

Thermochimica Acta 306 (1997) 143–151

thermochimica acta

Study of evaporation of organic pollutants by thermogravimetric analysis: Experiments and modelling

C. Pichon[a,b], V. Risoul[a,b], G. Trouvé[a], W.A. Peters[c], P. Gilot[a,*], G. Prado[a]

[a] *Laboratoire Gestion des Risques et Environnement, Ecole Nationale Supérieure de Chimie Mulhouse, Université de Haute Alsace, 25 rue de Chemnitz, 68200 Mulhouse, France*

[b] *Trédi, Département Recherche, Technopôle de Nancy-Brabois, B.P. 184-54505, Vandoeuvre lès Nancy, France*

[c] *Energy Laboratory and Center for Environmental Health Sciences, Massachusetts Institute of Technology, 77 Massachusetts Avenue, Cambridge, MA 02139, USA*

Received 3 June 1997; accepted 28 June 1997

Abstract

Evaporation of four pure organic compounds of interest as environmental contaminants, i.e., naphthalene, hexachlorobenzene (HCB), 4-chlorobiphenyl (4-CBP), and *n*-decane, was studied at constant heating rates of 5, 10, and 25°C/min by thermogravimetric analysis (TGA). The three aromatic solids began to evaporate at or below their melting point and were completely vaporised well below their boiling points. The extent of evaporation at a fixed temperature increased with decreasing heating rate and when pressure was decreased from 10^5 to 10^4 Pa. Evaporation during heat-up was modelled as one-dimensional mass transfer to the ambient gas, of vapor in equilibrium with liquid in the TGA crucible. The surface area of evaporating liquid and the thickness of the concentration boundary layer was respectively estimated from apparatus geometry, and by best fitting model predictions to isothermal evaporation data. CFD analysis of the boundary layer supported use of a 1-D, stationary boundary layer approximation. At 10°C/min the model predictions are in good agreement with experiment for evaporation of HCB and 4-CBP, but do not satisfactorily represent *n*-decane evaporation, apparently because of inadequate knowledge of the liquid surface area. The model captured well the observed effects of total pressure and the broad trends with changing heating rate. © 1997 Elsevier Science B.V.

Keywords: Evaporation; Organic pollutants; Naphthalene; Hexachlorobenzene; 4-chlorobiphenyl; *n*-decane; Thermogravimetric analysis

1. Introduction

Thermogravimetric Analysis (TGA) is a well-known technique to study physical or chemical phenomena that change the mass of a batch specimen. The time-wise continuous record, high resolution, and convenience of mass measurements under conditions offering good control of the substrate temperature, make TGA an appealing, widely used technique. For example, combustion-related phenomena in which oxidation consumes a sample have been studied [1–8]. Thus, kinetic constants for soot oxidation have been deduced from TGA data, using a mathematical model to account for limitations on oxygen mass transfer outside and within a bed of soot particles

*Corresponding author. Tel.: 00 33 3 89327655; fax: 00 33 3 68327661.

PII S0040-6031(97)00318-3

[5–8]. Other processes investigated by TGA include chemical decomposition of solids, e.g., decarbonation of $CaCO_3$ [9], and adsorption/(desorption) phenomena in which a sample gains/(loses) weight with time [10–13].

This work focuses on evaporation of organic compounds during heat-up and at a constant temperature. This work is motivated by a TGA study of soil thermal decontamination [14] which concluded that evaporation was a critical process in removal of 70% or more of the pollutant (pyrene). However, the measured evaporation rate of pure pyrene was about fivefold faster than the rate of pyrene removal from the soil at the same temperature [14]. Thus, further understanding of pure compound evaporation can elucidate underlying mechanisms of soil decontamination and provide new insights for process modeling and simulation. Accordingly, this paper provides data on the effect of temperature, heating rate, and total external pressure, on the extents of evaporation of four organic compounds, as well as a mathematical model for nonisothermal evaporation. The compounds, naphthalene, hexachlorobenzene (HCB), 4-chlorobiphenyl (4-CBP), and *n*-decane, are structurally complex and span a significant range of volatility. Their evaporation behavior is pertinent to soil cleanup and to the fate and transport of pollutants in process waste streams and ambient air, i.e., the dynamics of pollutant distribution between the vapor phase and various condensed phases, e.g., pure liquid, particulate-borne material.

2. Experimental

Experiments were conducted with a Cahn thermobalance which was operated with a gas-flow vertical. The initial sample mass was about 15 mg. Nearly hemi-spherical crucible, 4.5 mm of diameter and 5 mm deep, was used to contain the sample. The tests were conducted under a flow of 5 Nl/h of nitrogen. The operating temperatures ranged from 20 to 800°C. Different heating rates, from 5 to 25°C/min were used. Control experiments, i.e. under the same conditions, but without any compound within the crucible, were carried out to correct the measured mass for effects of variation in the balance calibration with temperature.

Some experiments were carried out isothermally by preheating the samples at 5°C/min to a particular operating temperature, based on previous experiments on soil decontamination. For isothermal runs, the weight loss was only recorded when the operating temperature was reached and this time was taken as time zero. In some experiments, the effect of the total pressure was investigated, particularly a reduced pressure of around 10^4 Pa.

Experiments were conducted with four pure organic contaminants: naphthalene, hexachlorobenzene (HCB), 4-chlorobiphenyl and *n*-decane. Experiments were at least repeated twice and good reproducibility was obtained.

3. Results

To illustrate typical data, thermograms for isothermal evaporation of 4-chlorobiphenyl at 160°C, HCB at 215°C, *n*-decane at 80°C and naphthalene at 100°C, are presented in Fig. 1. The weight loss appeared to be almost a linear function of time for the different pollutants except for HCB. From each thermogram, the maximum rate of weight loss, obtained at time zero, was evaluated and taken as the experimental evaporation rate.

The thermograms corresponding to the evapora tion of pure 4-chlorobiphenyl and HCB during heat-up at 10°C/min are presented in Figs. 2 and 3, respectively. For the 3.56 mg – sample of 4-chloro-

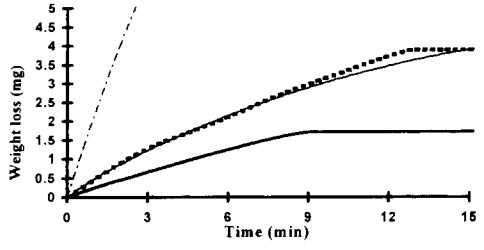

Fig. 1. Thermograms obtained under isothermal conditions. ——— 4-chlorobiphenyl, $m_i = 5.33$ mg and $m_0 = 3.73$ mg, temperature: 160°C; ——— HCB, $m_i = 6.99$ mg and $m_0 = 4.53$ mg, temperature: 215°C - - - naphthalene, $m_i = 6.11$ mg and $m_0 = 4.21$ mg, temperature: 100°C; – · – · *n*-decane, $m_i = 30.63$ mg and $m_0 = 9.29$ mg, temperature: 80°C. A mass of pollutant equal to $(m_i - m_0)$ was lost while heating each sample from room temperature to the stated isothermal temperature.

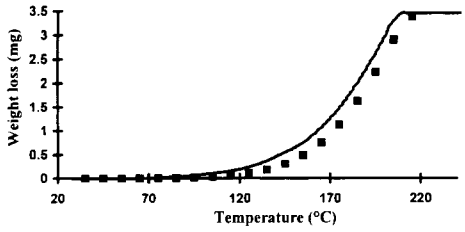

Fig. 2. Thermograms of 4-chlorobiphenyl obtained at 10°C/min; m_0 = 3.56 mg. ——— experiment; ■ model (h = 5.2 mm).

biphenyl, the weight loss begins at about 80°C, very close to the melting point (77.7°C) of the compound, and ends at about 200°C, far below its boiling point (291°C). For the 3.02 mg – sample of HCB (melting point: 228.5°C, boiling point: 309.8°C), the weight loss begins at about 160°C, corresponding to sublimation, and approaches completion at about 230°C.

The effect of heating rate was also investigated. Evaporation of 4-chlorobiphenyl and HCB was studied at 5, 10 and 25°C/min. The effect of the heating rate is quite important since the same extent of weight loss was obtained at a 20–30°C lower temperature when the sample was heated at 5°C/min instead of 25°C/min, as shown in Fig. 4 for the 4-chlorobiphenyl. The same trend was obtained with HCB, but was much less pronounced.

The effect of the operating pressure was investigated for the 4-chlorobiphenyl heated at 5°C/min. The thermograms obtained at 10^4 and 10^5 Pa are compared in Fig. 5. Beyond about 10% decontamination the temperature required for a given extent of weight loss is decreased by roughly 50°C when the pressure is decreased from 10^5 to 10^4 Pa.

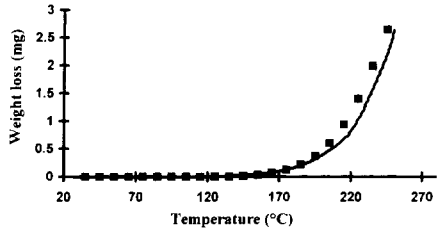

Fig. 3. Thermograms of HCB obtained at 10°C/min; m_0 = 3.02 mg. ——— experiment; ■ model (h = 8.1 mm).

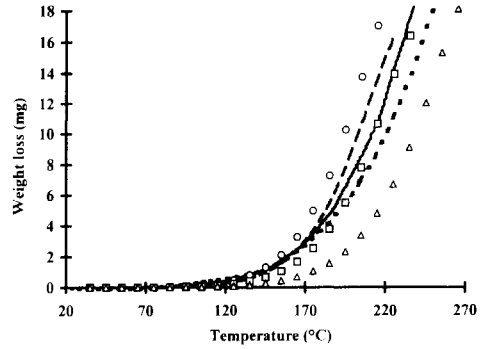

Fig. 4. Thermograms obtained for 4-chlorobiphenyl at 3 different heating rates. – – – experiment, 5°C/min, m_0 = 16.33 mg; ○ model, 5°C/min, m_0 = 16.33 mg, h = 5.2 mm; ——— experiment, 10°C/min, m_0 = 18.34 mg; □ model, 10°C/min, m_0 = 18.34 mg, h = 5.2 mm; - - - experiment, 25°C/min, m_0 = 18.57 mg; Δ model, 25°C/min, m_0 = 18.57 mg, h =5.2 mm.

4. Modelling

The evaporation process can be modelled with two main hypotheses:

- thermodynamic equilibrium between the liquid and its vapor at the liquid surface, which allows the mole fraction of pollutant vapor at the liquid surface to be determined,
- transport of the pollutant by convection and diffusion from the liquid surface to the outlet section of the reactor.

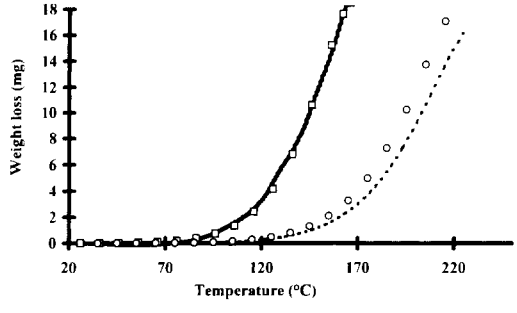

Fig. 5. Thermograms obtained, at 5°C/min, at two different operating pressures for 4-chlorobiphenyl ··· pressure 10^5 Pa, experiment, m_0 = 16.33 mg, ○ pressure: 10^5 Pa, model, m_0 = 16.33 mg, h = 5.2 mm; ——— pressure: 10^4 Pa, experiment, m_0 =18.52 mg; □ pressure: 10^4 Pa model, m_0 = 18.52 mg, h =4.7 mm.

In the following analysis, these two hypotheses are used first in a complete model of isothermal pollutant evaporation, using the CFD package FLUENT. The computed rate of evaporation is then compared to the experimental one. The results are then used to investigate if a simple one-dimensional transport model can be developed to be easily implemented in the more complex representation of the soil decontamination process.

5. Isothermal evaporation model

The following assumptions have been invoked for the pollutant mass transport:

- the gas flow is laminar and isothermal;
- the thermobalance reactor is cylindrical with a length of 31.0 cm upstream of the crucible which is provided for the development of the parabolic velocity profile for the thermobalance sweep gas;
- the crucible is a cylinder;
- the evaporation process is regarded as steady state;
- the area of the surface of the liquid on which evaporation takes place is estimated from the sample mass when the chosen temperature is reached, the density of the liquid at this temperature and the shape of the crucible. This area is taken as the cross-section of the crucible;
- the mole fraction of pollutant vapor at the liquid surface is obtained from the saturated vapor pressure P_{sat} of the pollutant at the given temperature: $y_{sat} = P_{sat}/P$
- the pollutant does not undergo chemical reaction during its evaporation or transport to the ambient (i.e. sweep) gas.

The temperature dependence of the saturated vapor pressures of naphthalene, *n*-decane and HCB are given by the following equation [15]:

$$P_{sat} = \exp\left(A + \frac{B}{T} + C\ \ln(T) + GT^{E}\right) \qquad (1)$$

In the case of 4-chlorobiphenyl, the Riedel equation [16] applies. This equation has the same form as Eq. (1) but relates the reduced vapor pressure (P_s/P_c) to the reduced temperature (T/T_c). P_c and T_c are the critical pressure and critical temperature, respectively. The values of the coefficients A, B, C, G and E are given in Table 1.

The diffusion coefficients D are estimated from their Lennard–Jones parameters [17] and their temperature dependence is represented by the function $D = aT^{1.5}$. The values of 'a' are listed in Table 1.

6. Results

FLUENT returned two main quantities, the flux density of the pollutant j_{fl} (kg m^{-2} s^{-1}) at the liquid surface and the bulk pollutant mass fraction y_b at the reactor outlet. The contours of the pollutant mass fraction are depicted in Fig. 6 for the case of HCB. Within the crucible, the contours are almost parallel and evenly spaced over most of its depth, meaning that diffusion was the main transport mechanism in that region. Near the mouth of the crucible, dilution of the pollutant by nitrogen made convective flow significant.

The density of the flux of the pollutant j_{fl} appeared to be non-uniform on the liquid surface. The evaporation rate R_{ev} over the whole surface could be evaluated with the following equation:

$$R_{fl} = \int_0^R 2\pi r j_{fl(r)} dr \qquad (2)$$

Table 1
Coefficients for estimation of the pollutant vapor pressure at saturation and coefficient for estimation of the pollutant diffusivity

Pollutant	Temperature range of application	A	$B/(K^{-1})$	C	$G/(K^{-E})$	E	$a/(m^2\ s^{-1}\ K^{-1.5})$
Naphthalene	353.43–748.35	85.29	-9.0622×10^{3}	−9.0648	3.5805×10^{-6}	2	1.303×10^{-9}
n-decane	243.51–618.45	121.25	-1.0115×10^{4}	−14.543	8.2302×10^{-6}	2	1.115×10^{-9}
HCB	501.70–825.00	353.98	-2.8327×10^{4}	−47.006	1.6001×10^{-5}	2	1.5999×10^{-9}
4-Clbiphenyl	?–815	12.2858	−12.6368	−6.796	0.351	6	1.0603×10^{-9}

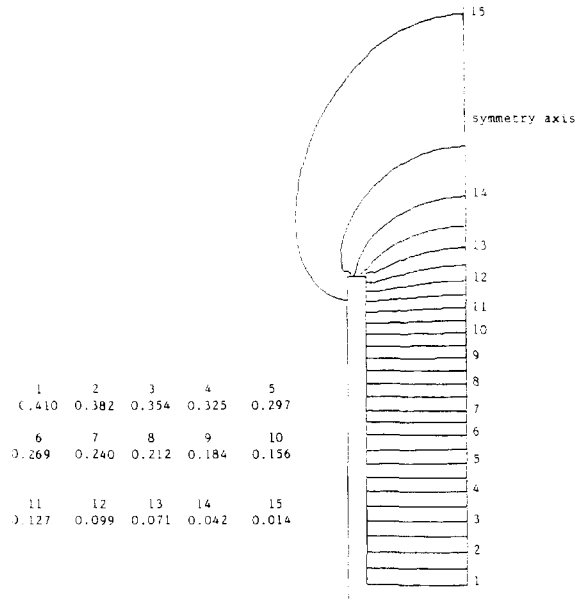

Fig. 6. Contours of HCB mass fraction computed by FLUENT at 215°C. Due to the symmetry, only half of the crucible is represented.

A mean value of j_{fl} was defined by

$$\bar{j}_{fl} = \frac{R_{fl}}{\pi R^2} \tag{3}$$

The area of the surface of the liquid appeared, as expected, to be a critical parameter. Unfortunately, this parameter was not known with high accuracy since the shape of the crucible was not exactly hemi-spherical and, due to capillary phenomena, the liquid surface was not a perfectly flat plane, normal to gravity. It was then decided to adjust the area of this evaporating surface to obtain better agreement between experimental and computed evaporation rates. A relative difference in the range 20–30% between this adjusted area and that calculated as described in the hypotheses was observed, except for decane (where the value was 148%).

The experimental and computed evaporation rates are given in Table 2, for every pollutant, as well as the relative variation ($\delta j_{fl}/\bar{j}_{fl}$) of the non-uniform density of the flux of every pollutant on the liquid surface. δj_{fl}, supplied by Fluent, is the difference between the maximum value of j_{fl} ($r = R$) and the minimum value ($r = 0$). The relative difference between the predicted and observed evaporation rates was less than 10% (see Table 2, column 5). The small relative variation of j_{fl} over the liquid surface (the maximum value is 12.7% for *n*-decane and falls to less than 1% for the other pollutants) allows the simplifying hypothesis of a uniform value of j_{fl} in a more simple model.

As a conclusion of this section, this previous isothermal model gave a good representation of the evaporation process, providing the area of the liquid surface was known with enough accuracy. It was not realistic to use such a detailed model to simulate evaporation during heat-up, i.e. in transient conditions. Since the flux density j_{fl} could be assumed as uniform over the liquid surface, modelling was attempted assuming a one-dimensional concentration boundary layer in which the pollutant was transported through a stagnant nitrogen atmosphere above the liquid surface as shown in Fig. 7. This hypothesis was reinforced by the fact that FLUENT showed that nitrogen did not penetrate deeply inside the crucible. Thus dilution of the pollutant by convective flow of nitrogen was assumed to occur only at the top of this layer where the mole fraction of the pollutant was the bulk x_b. This boundary layer made it possible to account for the effect of heating rate by means of an accumulation term in the mole balance equation.

Table 2
Experimental and computed evaporation rates under isothermal conditions. Relative variation of the density of the mass flux of pollutant over the liquid surface

Pollutant	Temperature (°C)	R_{ev}/(kg s^{-1})	R_{fl}/(kg s^{-1})	$\lvert R_{ev} - R_{fl}\rvert/R_{ev}$ (%)	$\delta j_{fl}/j_{fl}$ (%)
n-decane	80	1.42×10^{-8}	1.38×10^{-8}	2.9	12.7
Naphthalene	100	3.10×10^{-9}	2.93×10^{-9}	5.5	0.5
4-Clbiphenyl	169	3.51×10^{-9}	3.73×10^{-9}	6.2	0
HCB	215	7.20×10^{-9}	6.53×10^{-9}	9.3	0

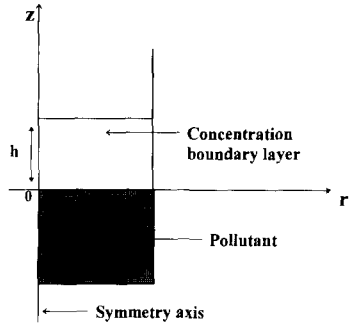

Fig. 7. Model geometry for the one-dimensional concentration boundary layer.

The first step was to estimate the thickness h of this boundary layer, for each pollutant, at a given isothermal temperature. The molar flux density of pollutant j_m (mol m^{-2} s^{-1}) was expressed by

$$j_m = -\frac{Dc}{(1-x)}\frac{dx}{dz} \quad (4)$$

in which c is the concentration ($c = P/RT$) and x the mole fraction of the pollutant.

The uniform value of j_m all over the thickness of the boundary layer led to the following equation

$$h = \frac{Dc}{j_m}\ln\left(\frac{1-x_b}{1-x_{sat}}\right) \quad (5)$$

Using the values of x_b and j_m obtained from the model (j_m is taken as $\bar{j}_{fl}$), the values of h were calculated. These values, together with the values of j_m, x_{sat} and x_b are given in Table 3 for every pollutant, at one or two temperatures. The thickness of the one-dimensional boundary layer appears to be of the same order of magnitude as the 5 mm depth of the crucible except for HCB at 215°C for which Eq. (4) gives about 8.1 mm. The calculated thicknesses increase with the evaporation temperature as shown in Table 3 for 4-chlorobiphenyl and HCB. This effect of temperature is more pronounced for HCB.

7. One-dimensional model of evaporation during heat-up

As for the isothermal evaporation model, equilibrium between the liquid and the vapor was assumed at the liquid surface leading to the knowledge of the mole fraction of pollutant vapor at the liquid surface. The transport was assumed to occur in a one-dimensional cylindrical concentration boundary layer with a cross-sectional area equal to the area of the liquid surface. This area was computed as a function of temperature because the pollutant surface area declined as evaporation proceeded.

As a first approximation, the thickness of the boundary layer was estimated at a mean temperature and kept constant during the whole process.

A mole balance within the concentration boundary layer led to Eq. (6) for transient conditions

$$\frac{\partial j_m}{\partial z} + Dc\frac{\partial x}{\partial t} = 0 \quad (6)$$

Using Eqs. (4) and (6), Eq. (7) was obtained for the pollutant mole fraction

$$\frac{1}{(1-x)^2}\left(\frac{\partial x}{\partial z}\right)^2 + \frac{1}{(1-x)}\frac{\partial^2 x}{\partial z^2} - \frac{\alpha}{D}\frac{\partial x}{\partial T} = 0 \quad (7)$$

Table 3
Data used for the estimation of the thickness of the pollutant concentration boundary layer and values of this thickness at different temperatures

Pollutant	*n*-decane	Naphthalene	4-Clbiphenyl	4-Clbiphenyl	HCB	HCB
Temperature/(°C)	80	100	120	160	180	215
h/mm	4.2	5.5	4.6	5.2	5.6	8.1
h^a/mm			4.7			21.8
j_m/(mol m^{-2} s^{-1})	2.39×10^{-3}	1.44×10^{-3}	2.34×10^{-4}	1.95×10^{-3}	7.90×10^{-4}	2.67×10^{-3}
x_{sat}	4.02×10^{-2}	2.46×10^{-3}	3.99×10^{-3}	3.42×10^{-2}	1.40×10^{-2}	6.40×10^{-2}
x_b	1.58×10^{-3}	3.79×10^{-4}	7.2×10^{-5}	3.24×10^{-4}	2.44×10^{-5}	4.08×10^{-4}

[a] ($P = 10^4$ Pa)

The boundary conditions are:

$$\text{at } z = 0,\ x = x_{sat} \tag{8}$$

$$\text{at } z = h,\quad x_b = -\frac{cDS}{F_{N_2}}\left(\frac{\partial x}{\partial z}\right)_{z=h} \tag{9}$$

This second condition expresses the continuity of the flux at the top of the concentration boundary layer. The initial condition is:

$$\text{at } t = 0,\quad x = x_{sat} \tag{10}$$

Time $t = 0$ corresponds to ambient temperature at the beginning of the heat-up process.

These equations were solved using a finite difference method with an implicit scheme. The number of nodes was 50 and the temperature step was 0.1°C.

This resolution returned the distribution of the pollutant mass fraction over the thickness of the concentration boundary layer. From the computed x_b value, the elementary weight loss dm corresponding to the temperature step dT was calculated by

$$dm = \frac{x_b}{(1 - x_b)}\frac{F_{N_2}M}{\alpha}dT \tag{11}$$

The weight loss was then calculated versus temperature, for 4-chlorobiphenyl, using $h = 5.2$ mm and for HCB, $h = 8.1$ mm, for a heating rate of 10°C min^{-1}. The curves obtained with the model are compared to experimental ones in Figs. 2 and 3, for 4-chlorobiphenyl and HCB, respectively. Agreement is satisfactory for both pollutants, showing that taking a mean value of the thickness boundary layer is a reasonable approximation. The same calculations were performed for the two other pollutants, but a correspondingly good agreement between model predictions and experiment was not obtained. For *n*-decane, the reason is probably that it was not possible to estimate the right value of the area of the liquid surface. For naphthalene, the thermograms obtained from the experiment were probably unreliable because during heat-up some naphthalene vapor condensed on the wire which suspends the crucible. It was not possible to estimate the mass of this deposited material.

The model was also used to simulate the effect of heating rate. For evaporation of the 4-chlorobiphenyl, the results obtained with the model are plotted in Fig. 4, together with the experimental results. Using the thickness of the concentration boundary layer previously calculated, $h = 5.2$ mm, good agreement was not obtained for every heating rate at all temperatures. Nevertheless, broad trends as well as the important phenomenon of increasing weight loss at a fixed temperature, with decreasing heating rate, are well captured by the model. More work is needed to explain the better overall agreement between the model and the data at the intermediate heating rate (10°C/min).

The model was also used to test the effect of the operating pressure on the evaporation of 4-chlorobiphenyl during heat-up at 5°C/min. The thickness of the concentration boundary layer at an operating pressure of 10^4 Pa was estimated at 120°C, using the one-dimensional isothermal model. This model returned a value of 4.7 mm, very close to the value of 5.2 mm calculated at a pressure of 10^5 Pa. The model predictions are compared with experiment in Fig. 5. Excellent agreement was obtained, building confidence in the validity of the model.

8. Conclusions

Thermogravimetric analysis is a useful and informative experimental technique for quantitative study of the evaporation of individual organic compounds, provided their vapor does not condense on the balance after volatilization. Heating rate and total pressure significantly affect evaporation. For example, the extent of vaporization at a fixed temperature, of four organic compounds of interest as environmental contaminants, i.e., naphthalene, hexachlorobenzene (HCB), 4-chlorobiphenyl (4-CBP), and *n*-decane, was found to decrease when heating rate was increased from 5, 10, and to 25°C/min, and to increase when pressure was decreased from 10^5 to 10^4 Pa.

Pure compound evaporation during heat-up can be simulated as one-dimensional mass transfer to the ambient gas, of vapor in equilibrium with liquid in the TGA crucible. For practical computations, the area of the evaporating liquid surface and the thickness of the concentration boundary layer between the liquid and the ambient gas, must be known throughout the volatilization process. These two parameters can be respectively estimated from apparatus geometry and

the best fitting model predictions to isothermal data on rates and extents of evaporation as affected by temperature. CFD analysis of the boundary layer flow supports use of a 1-D, stationary boundary layer approximation. The model, although simple, well captures the observed effect of operating pressure, and is also able to predict the overall trends when heating rate is varied between 5 and 25°C/min. The model is expected to be a useful subsystem module to account for evaporation/condensation kinetics in more complex simulations. Examples are thermal desorption of contaminants from soil, and partitioning of pollutants between vapor and condensed phases (i.e. liquid, particulate-borne) in process streams and ambient air.

9. List of symbols

c	gas concentration/(mol m^{-3})
D	diffusion coefficient of the pollutant in the gas phase/(m^2 s^{-1})
F_{N_2}	nitrogen flow rate/(mol s^{-1})
h	thickness of the concentration boundary layer/m
j_{fl}	density of the mass flux of the pollutant computed by FLUENT/(kg m^{-2} s^{-1})
$\bar{j}_{fl}$	mean value of the density of the mass flux of the pollutant computed by FLUENT/(kg m^{-2} s^{-1})
j_m	density of the molar flux of the pollutant/(mol m^{-2} s^{-1})
m	mass of the pollutant remaining in the crucible at time t/kg
mi	initial mass of the pollutant deposited within the crucible/kg
m_0	mass of the pollutant in the crucible at time 0/kg
M	molecular weight of the pollutant/(kg mol^{-1})
P	operating pressure/Pa
P_c	critical pressure of the pollutant/Pa
P_{sat}	pollutant vapor pressure at saturation/Pa
r	cylindrical coordinate/m
R	radius of the liquid surface/m
R_{ev}	experimental evaporation rate of the pollutant/(kg s^{-1})
R_{fl}	evaporation rate of the pollutant calculated by FLUENT/(kg s^{-1})
S	cross sectional area of the cylindrical concentration boundary layer/m^2
t	time/s
T	operating temperature/K
T_c	critical temperature of the pollutant/K
x	pollutant mole fraction
x_b	bulk pollutant mole fraction
x_{sat}	mole fraction of the pollutant in the vapor phase in equilibrium with the liquid
y_{sat}	mass fraction of the pollutant in the vapor phase in equilibrium with the liquid
z	vertical ordinate/m

10. Greek symbols

α	heating rate/(K min^{-1})

Acknowledgements

We thank TREDI and the French "Ministère de l'Industrie" for financial support of this project. Support of research at MIT on soil thermal decontamination by NEHS Grant No. ES04675 (MIT Superfund Hazardous Substances Basic Research Program) is also gratefully acknowledged.

References

[1] V. Šatava, J. Thermal Anal., 5 (1973) 217.
[2] O. Carp, E. Segal, Thermochim. Acta 185 (1991) 111.
[3] D. Garn, Thermochim. Acta 135 (1988) 71.
[4] L. Tognotti, A. Malotti, L. Petarca, S. Zanelli, Combust. Sci. and Technol. 44 (1985) 15.
[5] P. Gilot, F. Bonnefoy, F. Marcuccilli, G. Prado, Combust. Flame 95 (1993) 87.
[6] F. Marcuccilli, P. Gilot, B.R. Stanmore and G. Prado, Twenty-Fifth Symposium (International) on Combustion, The combustion Institute, Pittsburg, 1994, p. 619.
[7] B.R. Stanmore, P. Gilot, Thermochim. Acta 261 (1995) 151.
[8] P. Gilot, A. Brillard, B.R. Stanmore, Combust. Flame 102(4) (1995) 471.
[9] A. Palandri, P. Gilot, G. Prado, J. of Anal. Pyrol. 27 (1993) 119.
[10] G. Hakvoort, Thermochim. Acta 233 (1994) 63.
[11] M. Guyon, B.R. Stanmore and P. Gilot, Chem. Commun., (1996) 1227.

[12] S. Han, Chlorocarbon, Transport Out of Contaminated Soil Particles, S.M. Thesis, Dept. of Civil and Engineering, MIT, Cambridge, MA, 1994.
[13] T.F. Lin, J.C. Little, W.W. Nazaroff, Environ. Sci. Technol. 28(2) (1994) 322.
[14] P. Gilot, W.A. Peters, J.B. Howard, Environ. Sci. and Technol. 31(2) (1997) 461.
[15] T.E. Daubert and Dauner R.P., Physical and Thermodynamic Properties of Pure Chemicals. Data Compilation, Taylor and Francis, 1989.
[16] The Properties of Gases and Liquids, McGraw-Hill Book Company, R.C. Reid, J.M. Prausnitz and J.M. Sherwood (Eds.), 1977.
[17] The Role of Diffusion in Catalysis, C.N. Satterfield, T.K. Sherwood (Eds.), Addison-Wesley Publishing Company Inc., 1963, p. 5–10.